Hindawi
Journal of Chemistry
Volume 2020, Article ID 3297184, 9 pages
https://doi.org/10.1155/2020/3297184

Research Article

Ultrasonic-Assisted Synthesis and Characterization of Chitosan-Graft-Substituted Polyanilines: Promise Bio-Based Nanoparticles for Dye Removal and Bacterial Disinfection

Mutairah Shaker Alshammari,[1] **Amr A. Essawy**,[1,2] **A. M. El-Nggar**,[3] **and S. M. Sayyah**[3]

[1]*Chemistry Department, College of Science, Jouf University, P.O. Box 2014, Sakaka, Aljouf, Saudi Arabia*
[2]*Chemistry Department, Faculty of Science, Fayoum University, 63514 Faiyum, Egypt*
[3]*Polymer Research Laboratory, Chemistry Department, Faculty of Science, Benisuef University, 62514 Benisuef, Egypt*

Correspondence should be addressed to Amr A. Essawy; aaessawy@ju.edu.sa

Received 13 November 2019; Accepted 2 January 2020; Published 31 January 2020

Guest Editor: Mohammad Saad Algamdi

The sonication-mediated oxidative-radical copolymerization using ammonium persulfate in acidic medium provides a new successful avenue to graft Chitosan with three methylaniline derivatives. The synthesized Chitosan-graft-polymethylanilines (CGPMA) were characterized using FTIR, UV-vis diffuse reflectance spectroscopy, XRD, thermogravimetric analysis (TGA), elemental analysis, and transmission electron microscopy (TEM). XRD spectra revealed that CGPMA have a higher crystallinity degree compared to the pristine Chitosan. In addition, a methyl position-dependent crystallinity is noticeable for the grafted copolymers. This could be confirmed from TEM images that reflect structure-affected morphologies of different ordering for the graft spherical nanoparticles. Interestingly, the copolymers prepared under ultrasonic irradiation show a high potency in dye uptake compared to nonsonicated ones. Moreover, an antibacterial preliminary test on the as-prepared materials was accomplished. We have achieved promising results, which encourages us to conduct more studies to process these materials in developing biomedical active composites.

1. Introduction

Recently, conducting polymers have taken a great consideration in the field of scientific research, especially in material science. Among conductive polymers, either polyaniline (PANI) or its derivatives are unique materials in many aspects such as handy preparation, considerable stability, and favored electrochemical features including the magnificent conduction mechanism and their wonderful optical, electrical, and catalytic properties [1]. However, polyaniline has a lack of process ability; this drawback was overcome either by protonation with suitable reactive acids or by preparation of polymer derivatives. The polymer deriving can be achieved through replacing hydrogen atoms either at nitrogen atom or in the aromatic rings of the polymer by active substituents [2]. PANI has promising applications in many fields, for example, rechargeable batteries, protection of metals against corrosion, gas-separation membranes, and molecular sensors [3, 4]. It is catchy and commercialized owing to its facile preparation, due to electrochemical or chemical processes and inexpensive production in large quantities [5]. It offers great environmental, chemical, and thermal stability [6]. PANI can be converted into protonated or deprotonated form via processing with acids or bases. The emeraldine salt of PANI is an acid doped conducting polymer, and its emeraldine base is an insulator polymer [7]. PANI also shows high antibacterial properties [8, 9].

Chitosan is a naturally occurring, biodegradable, nontoxic, nonallergenic biopolysaccharide derived from chitin, found abundantly in nature [10, 11]. Chitosan exhibits a broad particle use in many fields; it is a friable substance

which has a tendency to absorb some moisture. In addition, it is relatively inexpensive and of high molar mass with interesting physiochemical features [12].

The grafting of Chitosan could be achieved through the introduction of functional derivatives onto Chitosan via covalent bonding [13]. The grafting process on Chitosan is one of the routes to improve its characteristics, for example, enhancing chelation [14] or antibacterial impact [15] or boosting adsorption characteristics [16].

Chitosan and water insoluble Chitosan derivatives have a high adsorption power against toxic, fatty acids and dangerous heavy metal ions like Sn^{2+} and Sn^{4+} of inorganic or organic confinement, Hg^{2+}, Pb^{2+}, U^{6+}, and transition metal ions such as Ni^{2+}, Cu^{2+}, V^{4+}, Cd^{2+}, Cr^{3+}, and Zn^{2+} [17]. Chitosan and its derivatives have unique applications in biological field, such as antibacterial agents.

Recently, nanomaterials, including metallic, inorganic, and polymeric substances with a size of 1–100 nm, have attracted an increasing attention of many scientific interests [18]. Ultrasonication could result in new chemical reactivity within promoted reaction rate and thus reveals a new directory in chemistry, that is, sonochemistry [19]. In particular, sonochemistry that depends on highly intense ultrasound provides mediation to promote chemical reactions. The activation effect refers to the crushing, dispersion, and emulsifying processes that prevent particle aggregation and minimize its size. This enables particle preparation within a better and controlled shape, especially on the solid material, such as polyaniline [20]. In addition, the simplicity and safety of the sonochemical technique positioned it as a powerful tool in the field of green chemistry [21].

Therefore, this work presents a new avenue implying ultrasound mediated oxidative-radical copolymerization to graft the polysaccharide, Chitosan, with three methylaniline derivatives. The optimized grafting copolymerization parameters were studied. Interestingly, the as-prepared grafted copolymers exhibit structure-affected crystallinity, uniformity, and thermal stability. The preliminary test reveals potent adsorptivity to Remazol Red RB 133 (RR), a commonly used water-soluble azo dye. A crucial rule for ultrasonication in improving the grafted copolymer adsorptivity has been indicated by comparing the adsorption capacity of sonicated grafted copolymers with nonsonicated ones. Furthermore, the developed grafted copolymers were investigated for their efficacy in bacterial disinfection. Extensive studies on these applications will be conducted in further work.

2. Experimental

2.1. Materials and Methods. N-Methylaniline (NMA), 2-Methylaniline (2MA), and 3-Methylaniline (3MA) (Sigma Aldrich). Starting with the shrimp shells, Chitosan was extracted according to the methodology described in literature [22, 23] (M. Wt. ~109,000; deacetylation degree >85%). Ammonium persulfate and N-methyl-2-pyrrolidone (Loba Chemie, India) and acetic acid, hydrochloric acid, and acetone were supplied from El-Nasr Chemical Co. (Egypt). The azo dye, Remazol Red 133 of commercial grade, was used as received.

2.2. Synthesis of CGPMA. Chitosan solution (1.0 g/L) was prepared by adding appropriate Chitosan amount to acetic acid solution (2%) in a flask and stirring for 2 hours at room temperature (25°C ± 2). A mixture solution of substituted aniline solution (1.0×10^{-2} mol/L) and HCl (0.2 mol/L) was added to the solution of Chitosan at 5°C, under continuous stirring for 20 min. Ammonium persulfate (7.5×10^{-2} mol/L) in HCl (0.2 mol/L) was put drop-wisely to the mixture and the mixture was stirred for 5 hours at 5°C. Over the suite of polymerization, ultrasonic irradiation of the reaction course is employed by using an ultrasonic processor of 120 W and 38 kHz. The final admixture was separated, and the resulting precipitate was leached with deionized water, N-methyl-2-pyrrolidone, and acetone, respectively, to remove possibly present impurities, that is, monomers residue, initiator, and homopolymers chains; then, it was finally dried for 24 hours in a vacuum oven at 50°C.

It is important to mention that the prepared grafted copolymers are insoluble in almost all solvents either on cold or by heating. The grafting percentage was calculated by

$$\text{Grafting (G)\%} = \left(\frac{W - W_o}{W_o}\right) \times 100, \quad (1)$$

where W = the weight of CGPMA and W_o = the weight of original Chitosan.

2.3. Instrumental. FTIR spectra were measured on an IR spectrometer, Shimadzu model Affinity-1S. The diffuse reflectance spectroscopy along the ultraviolet-visible range was recorded on a Shimadzu Japan 3101 p spectrophotometer. X-ray of wavelength (1.54 Å) within a Cu detector in the X-ray diffractometer (D/Max2500VB2+/Pc, Rigaku Company) was employed to conclude the graft crystallinity. For TEM analysis, samples were taken on (JEOL, JEM-2100, Japan). The thermogravimetric analysis of the polymers was conducted using an Netzsch TGA 204 (Germany) in the presence of an N_2 atmosphere from 25°C to 600°C. A CHN Perkin-Elmer analyzer (USA) was used to address the elemental analyses of the developed grafts. A spectrophotometer (Agilent Cary 60) was used to monitor the absorption profile in the UV-vis range.

3. Results and Discussion

3.1. Characterization of the Grafted Chitosan. Representative sonicated CGPMA samples were distinguished by reflectance spectroscopy, FTIR, TEM, XRD, TGA, and elemental analysis.

3.1.1. FTIR Spectra. The IR spectroscopy shows a viable role for confirming the grafting copolymerization between Chitosan and substituted polyanilines.

The IR spectra of Chitosan and CGPMA were depicted in Figure 1. As seen for Chitosan, the overlapping due to NH_2

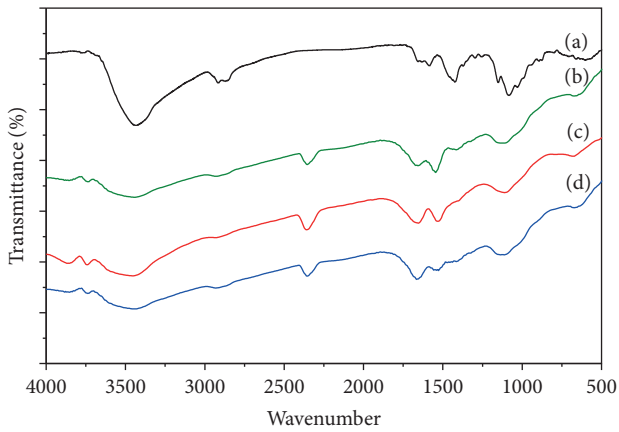

Figure 1: FTIR spectra of (a) Chitosan, (b) CGPNMA, (c) CGP2MA, and (d) CGP3MA.

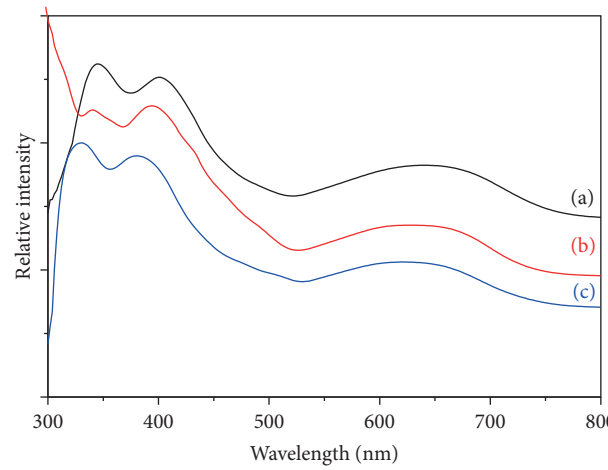

Figure 2: UV-vis diffuse reflectance spectra of (a) CGPNMA, (b) CGP2MA, and (c) CGP3MA.

and OH stretching vibrations resulted in the peak assigned at 3438 cm^{-1}, while the peaks found in the range of 2870–2920 cm^{-1} could be related to the symmetric–CH stretching. Moreover, the peak assigned at 1589 cm^{-1} is rendered to bending of NH_2 [24] and the peak assigned at 1426 cm^{-1} is related to the–CH_2 bending [22]. The revealed peak at 1154 cm^{-1} is due to the C–O–C bridge antisymmetric stretching, while that indicated at 1085 cm^{-1} is assigned to the C–O skeletal stretching vibration that are characteristics of the saccharide structure of Chitosan [25].

The IR spectra of Chitosan-graft-substituted polyanilines confirm the effective grafting of substituted polyanilines on Chitosan by the peaks at 1612, 1610, and 1607 cm^{-1} for CGPNMA, CGP2MA, and CGP3MA, respectively, owing to the distinctive peaks of quinonoid nitrogen (Q) and the peaks manifested at 1497, 1494, and 1493 cm^{-1} for CGPNMA, CGP2MA, and CGP3MA, respectively, accompanied by the benzenoid ring present in the substituted polyaniline. The peaks found at 1329, 1328, and 1326 cm^{-1} for CGPNMA, CGP2MA, and CGP3MA, respectively, are related to the C–N and C=N stretching vibration in substituted polyanilines [26, 27]. Additionally, the peak of N = Q = N bending vibrations of substituted polyaniline was indicated around 1150 cm^{-1} [28, 29]. Further, the shift of these peaks to lower wavenumber 1112, 1108, and 1106 cm^{-1} for CGPNMA, CGP2MA, and CGP3MA, respectively, was owing to hydrogen bonding between Chitosan and substituted polyanilines [30].

3.1.2. UV-Vis Diffuse Reflectance Spectra. The UV-vis DRS of the CGPMA are shown in Figure 2. The conductive polymers have some usual transitions in the UV-visible region, such as π-π^*, polaron-π^*, and π-polaron transitions, respectively. CGPMA (with aniline pattern) are predicted to have three peaks in the range of 320 nm, 400 nm, and 600–620 nm; the first absorption peak comes from π-π^* electron transfer in the benzenoid fragments, while the second and third absorption bands are due to the development of conducting polarons (quinoid segments), respectively, which are characteristics of the protonated type of substituted polyaniline [31].

In general, extending the double bond conjugation along the polymeric chain reveals a π-π^* energy difference decrease that corresponds to an increase in the wavelength indicating the interaction of Chitosan with substituted polyanilines. The recorded UV-vis spectra of CGPMA show that peaks of π-π^* excitation have been transferred from 321 to 351 nm, 346 nm, and 338 nm for CGPNMA, CGP2MA, and CGP3MA, respectively; moreover, the peaks assigned at ≈400 nm and 600–620 nm were transferred to around 406 nm and 650 nm [32, 33]. There are no significant absorption peaks for Chitosan in CGPMA spectrum that is expected at 330 nm which is related to the glucopyranoside structure of Chitosan because of overlapped benzenoid moieties of the grafted substituted polyanilines around 350 nm [34].

3.1.3. XRD Diffraction Patterns. Figure 3 displayed the XRD of chitosan and CGPMA. For the grafted Chitosan, the XRD spectra showed crystallinity from 20°–32° due to the grafting of substituted polyanilines onto the Chitosan backbone, whereas X-ray diffractogram of Chitosan showed amorphous pattern [30]. The crystallinity was noticeably amended due to hydrogen bonding interactions of inter- and intramolecular nature [35]. The XRD patterns b and especially c, d in Figure 3 show sharp and well defined peaks, which indicate the crystalline nature of CGPMA. Furthermore, the degree of crystallinity of CGP3MA and CGP2MA is noticeably higher than that of CGPNMA. This order of crystallinity of three different grafted copolymers can be explained according to the correlation between crystallinity and thermal stability shown in TGA results, similar to trends reported in literatures [36, 37]. This is due to a considerable localization of the electrons over the polymeric chain that leads to a decrease in the crystallinity [38–40]. The increasing localization depending on the methyl group position on the aniline monomer in the order: N-position, ortho-position, and meta-position leads thereby to the resulting order of crystallinity [39].

3.1.4. Transmission Electron Microscopy (TEM). In the present study, TEM images show the morphological features

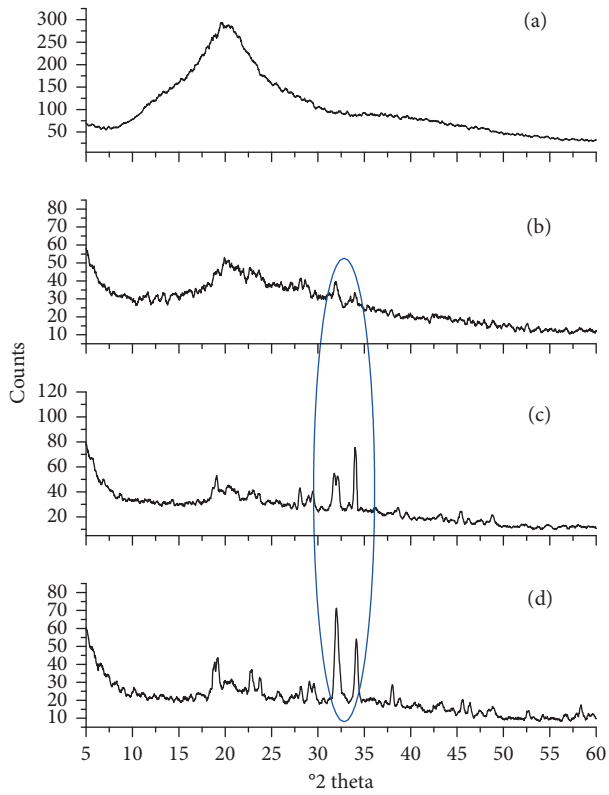

Figure 3: XRD spectra of (a) Chitosan, (b) CGPNMA, (c) CGP2MA, and (d) CGP3MA.

and surface appearance of Chitosan and CGPMA. Chitosan is shown in a network shape but CGPMA are shown as spherically shaped, smooth-surface nanoparticles of size range 2.8–16 nm as depicted in Figure 4. These features could be attributed to the added value of the applied ultrasonication along with the grafting process. The ultrasonication exerts immense shocking of ultrasonic waves, resulting in functionalities of dispersion, pulverization, and emulsification, revealing smaller particles within steady matrix [18].

3.1.5. Thermogravimetric Analysis (TGA). The thermal resistance of CGPMA was investigated taking the thermogravimetric behavior of Chitosan as a reference. TGA curves of Chitosan and CGPMA samples are displayed in Figure 5. First weight losses of all the samples (6–9%) observed between 30 and 100°C could be due to the loss of water content. Chitosan offers a distinct weight loss at 270–320°C, assigned to the decomposition of Chitosan chains. The residue for Chitosan at 600°C was 39%. The weight loss of CGPMA in the range of 100–240°C is corresponding to dopant molecules removal from the grafted copolymer structure. In the subsequent stage, the weight loss appeared between 220 and 390°C of CGPMA owing to the degradation of the CGPMA chain. About 8–14% of loosed weight within temperature gradient (400–600°C) was estimated for grafted copolymer due to the loosing of Chitosan side chain. At the end of the experiment at 600°C, nearly 56, 52 and 49% of CGP3MA, CGP2MA, and CGPNMA, respectively, remained as residue while, for Chitosan, 39% remained as a residue showing the greater thermal stability of CGPMA over Chitosan owing to the introduction of substituted polyanilines into Chitosan. Comparing the thermal stability of samples, Chitosan shows the highest foremost decomposition temperature (270–320°C), while CGPMA possess a higher residual amount and decompose at a relatively higher temperature (600°C) than Chitosan. This indicates that CGPMA have a relatively higher thermal stability than pure Chitosan perhaps due to an improvement in the intramolecular and intermolecular H-bonds in the structural skeleton of the copolymer [26, 41]. These findings are greatly compatible with results concluded from XRD and TEM analyses.

3.1.6. Elemental Analysis. Table 1 shows Chitosan elementary analysis, CGPMA, and the corresponding estimates of grafting percent (G%). Comparing elemental analysis of Chitosan with those of CGPMA indicated a noticeable increase in carbon and nitrogen contents as the monomer weight fraction was increased. These findings are consistent with G%.

3.2. Preliminary Study of Adsorption Process. We conducted a preliminary study to investigate the adsorption effect of Ch-g-PNMeANI as an example of Ch-g-MPANI copolymers. In a batch of experiments, fixed adsorbent amounts were added to 75 mL of RR solution (60 mg/L) in Erlenmeyer flask of 100 mL, which was then concussed using a horizontal shaker at 25 ± 2°C. The uptake of Remazol Red dye

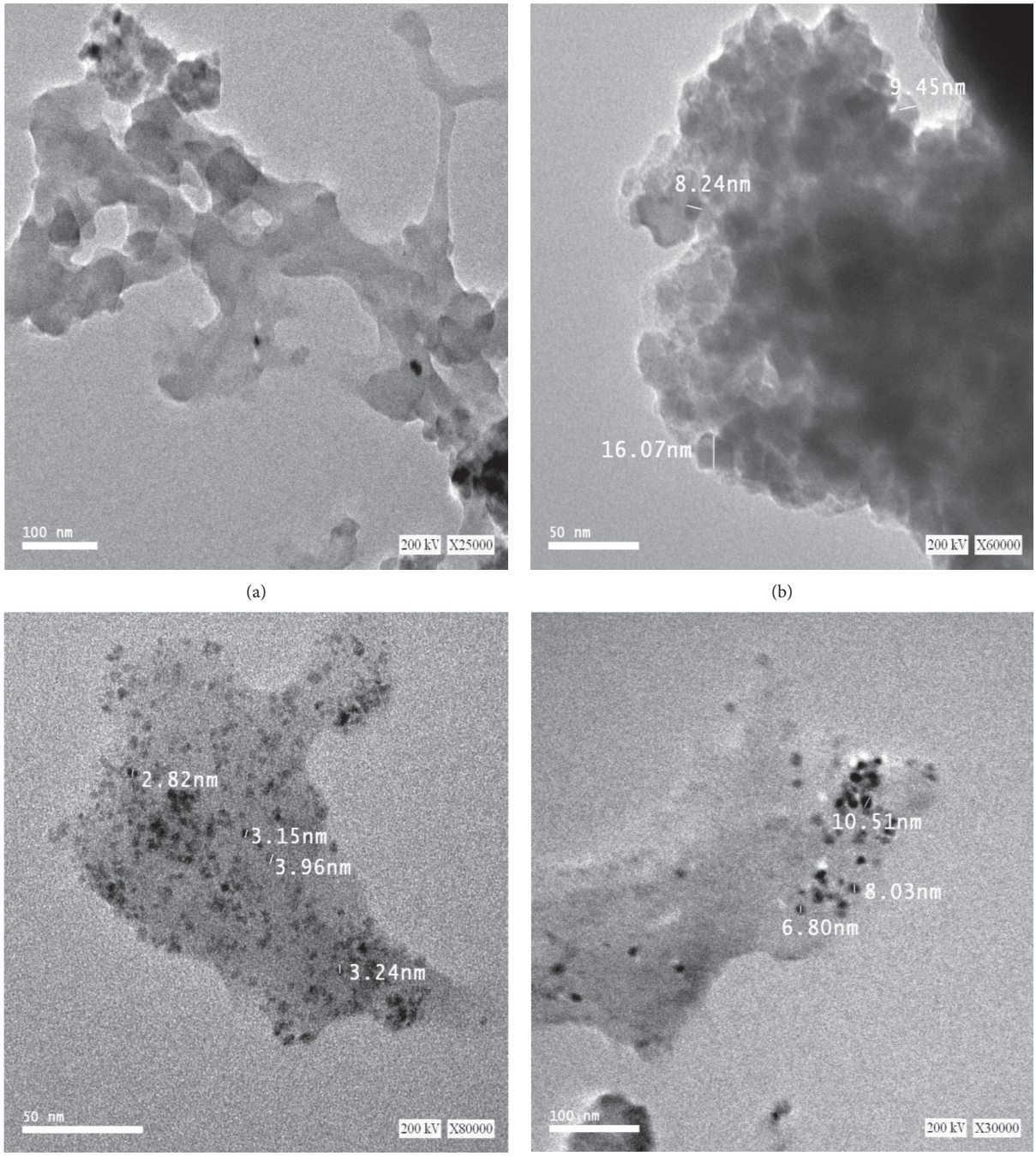

Figure 4: TEM images of (a) Chitosan, (b) CGPNMA, (c) CGP2MA, and (d) CGP3MA.

from aqueous solution in the adsorption process is shown in Figure 6(a). The adsorbent was isolated and the residual dye was analyzed via ultraviolet-visible absorption spectrophotometry at $\lambda_{max} = 520$ nm at different contact times, as shown in Figure 6(b). According to the calibration plot, the amount of dye sequestration by the adsorbents was estimated from (2):

$$q = \frac{\left[\left(C_o - C_f\right) \times V\right]}{m}, \quad (2)$$

where q is the sequestered amount of dye due to adsorbents (mg/g), C_o is the concentration of RR initially allowed to be contacting to the adsorbent (mg/L), C_f is the [dye] (mg/L) after the removal operation, V is the volume of dye solution (L) allowed to be contacting to the adsorbent, and m is the adsorbent mass (g). It can be seen that the characteristic absorption band of RR around 520 nm decreased rapidly with increasing the adsorption time and finally nearly disappeared in about 50 min. It is important to point out that the Ch-g-PNMeANI prepared using the developed synthetic

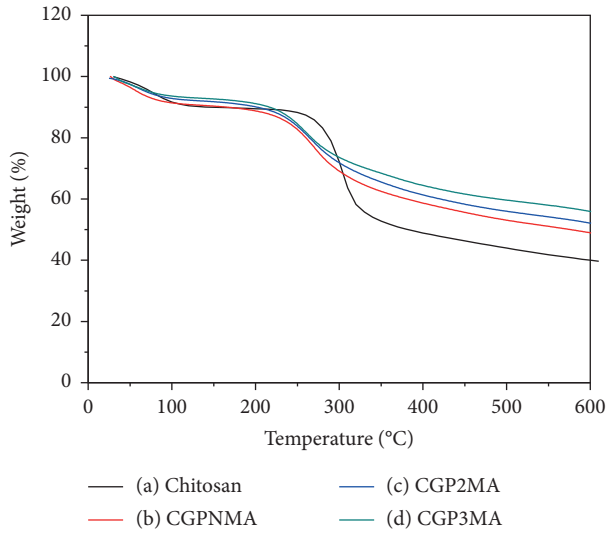

Figure 5: TGA of (a) Chitosan, (b) CGPNMA, (c) CGP2MA, and (d) CGP3MA.

Table 1: The elemental analysis of Chitosan and CGPMA and the calculated grafting percent.

Material	Grafting (%)	C (%)	H (%)	N (%)
Chitosan	—	39.88	4.63	6.30
CGPNMA	196	53.98	5.90	10.60
CGP2MA	187	43.42	6.37	8.60
CGP3MA	179	40.81	5.97	7.36

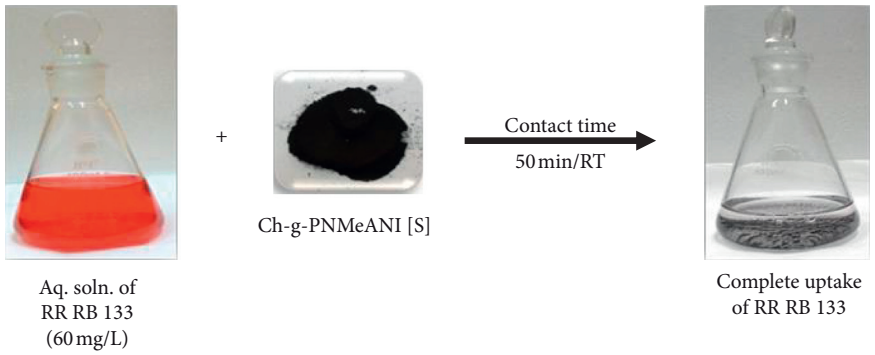

(a)

Figure 6: Continued.

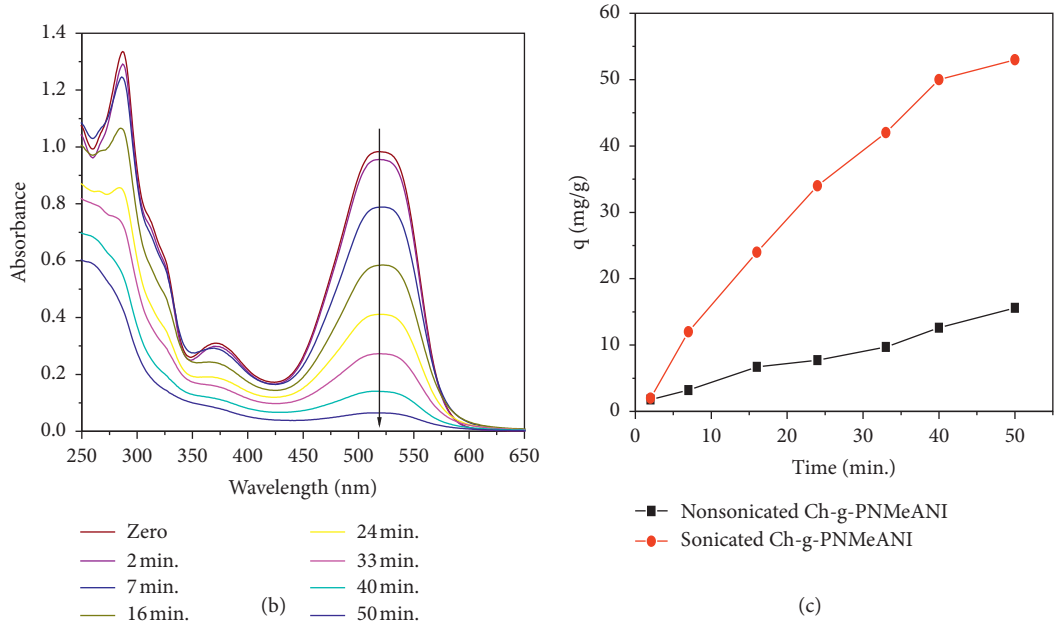

Figure 6: (a) Image shows the complete uptake of RR by Ch-g-PNMeANI adsorbent. (b) Adsorption-induced changes of the absorption spectrum of RR after different contact times with Ch-g-PNMeANI. (c) The variation of adsorption capacity with adsorption time for aqueous solution of RR dye onto nonsonicated (black line) and sonicated (red line) Ch-g-PNMeANI.

route is highly adsorptive and practically adsorbs all RR (60 mg/L), referring to a promising nanoparticle for water detoxification. On the other hand, the same weight from the nonsonicated Ch-g-PNMeANI has much lower adsorption capacity compared to the sonicated one, although all experimental conditions were the same, as shown in Figure 6(c). This interestingly highlights the crucial rule of ultrasonication in developing materials of highly desirable properties that maximize the environmental impact of the presented copolymers. More in-depth studies on this application will be under focus of further work.

3.3. Preliminary Study of Antibacterial Activity. A preliminary investigation was carried out to evaluate the antibacterial effect of CGPNMA as an example of CGPMA copolymers versus *Escherichia coli* (Gram-negative) in addition to *Staphylococcus aureus* (Gram-positive) that are provided from reference collection by determining the growth inhibitory effect of CGPNMA in broth bacterial suspension (10^8 CFU/mL) as a reference to quantify the initial colony that is employed in the plate counting method to be determined. The spectrophotometric analysis was conducted to quantify the CFU via the comparison of absorption optical density of standard CFU with unknown CFU at wavelength 625 nm. In a typical procedure, within an absorption range of optical density (0.08–0.13) due to McFarland standard 0.5 ($1\text{-}2 \times 10^8$ CFU/mL), the absorbance will be adapted by appropriate addition of sterilized distilled water. Then, the bacterial suspension (10^8 CFU/mL) was directly enrolled in the antibacterial tests for CGPNMA. In a sterilized Erlenmeyer flask, CGPNMA (0.1 g) was added to 10 mL of the bacterial suspension. Next, the flask was shaken for 2 hours at 250 rpm, and then 1.0 mL of this mixture was used to determine the change in the absorption optical density [42, 43]. The growth inhibitory % was counted as follows:

$$\text{Inhibition \%} = \frac{(\text{Control conc.} - \text{Test conc.})}{\text{Control conc.}} \times 100. \quad (3)$$

The CGPNMA composite NPs were tested for antibacterial activity by addressing the inhibition % of bacterial growth where estimates of 87% and 92% are recorded for *S. aureus* and *E. coli*, respectively. Such promising antibacterial potentiality could be attributed to the synergism within the conductive polymeric poly N-methylaniline grated onto the Chitosan skeleton [41]. More in-depth studies on this application will be under focus of further work.

4. Conclusions

CGPMA were prepared via the sonication-mediated chemical oxidation. FTIR ascertained Chitosan grafting by substituted polyanilines. Compared to the pristine amorphous Chitosan, the degree of crystallinity for both CGP3MA and CGP2MA is higher than CGPNMA that is attributed to the inter- and intramolecular hydrogen bonding. TEM analysis of CGPMA confirmed the presence of nanoparticles that have a nearly spherical shape and smooth surface. These features could result from the added value of ultrasonication along with the grafting process. Moreover, all grafted copolymers reveal a higher final degradation temperature than Chitosan. Furthermore, the provided new sonication-mediated synthetic route of the grafted copolymers results in high potency for dye uptake compared to the nonsonicated ones. Moreover, the

developed polymeric composites show promising antibacterial properties for both Gram-negative and Gram-positive bacteria. Thus, the developed sonicated-assisted synthetic route maximizes the environmental impact of the presented copolymers in either detoxification or disinfection of dye/bacterial enriched wastewaters.

Data Availability

The original data of this manuscript will be available upon request from the corresponding author.

Conflicts of Interest

The authors declare that they have no conflicts of interest.

References

[1] A. A. M. Farag, A. Ashery, and M. A. Shenashen, "Optical absorption and spectrophotometric studies on the optical constants and dielectric of poly (o-toluidine) (POT) films grown by spin coating deposition," *Physica B: Condensed Matter*, vol. 407, no. 13, pp. 2404–2411, 2012.

[2] Z. H. Wang, A. Ray, A. G. MacDiarmid, and A. J. Epstein, "Electron localization and charge transport in poly(o-toluidine): a model polyaniline derivative," *Physical Review B*, vol. 43, no. 5, pp. 4373–4384, 1991.

[3] H. Karami, M. F. Mousavi, and M. Shamsipur, "A new design for dry polyaniline rechargeable batteries," *Journal of Power Sources*, vol. 117, no. 1-2, pp. 255–259, 2003.

[4] P. P. Sengupta, S. Barik, and B. Adhikari, "Polyaniline as a gas-sensor material," *Materials and Manufacturing Processes*, vol. 21, no. 3, pp. 263–270, 2006.

[5] S. M. Sayyah, A. A. Aboud, A. B. Khaliel, and S. M. Mohamed, "Oxidative chemical polymerization of ortho-tolidine in acid medium using $K_2Cr_2O_7$ as oxidizing agent and characterization of the obtained polymer," *International Journal of Advanced Research*, vol. 2, no. 6, pp. 586–607, 2014.

[6] J. Prokeš and J. Stejskal, "Polyaniline prepared in the presence of various acids: 2. Thermal stability of conductivity," *Polymer Degradation and Stability*, vol. 86, pp. 187–195, 2004.

[7] P. K. Kahol, K. K. Satheesh Kumar, S. Geetha, and D. C. Trivedi, "Effect of dopants on electron localization length in polyaniline," *Synthetic Metals*, vol. 139, no. 2, pp. 191–200, 2003.

[8] M. R. Gizdavic-Nikolaidis, J. R. Bennett, S. Swift, A. J. Easteal, and M. Ambrose, "Broad spectrum antimicrobial activity of functionalized polyanilines," *Acta Biomaterialia*, vol. 7, no. 12, pp. 4204–4209, 2011.

[9] S. H. I. Nanlin, X. Guo, H. Jing, J. Gong, C. Sun, and K. Yang, "Antibacterial effect of the conducting polyaniline," *Journal of Materials Science and Technology*, vol. 22, pp. 289-290, 2009.

[10] K. Aoi, A. Takasu, and M. Okada, "New chitin-based polymer hybrids. 2. Improved miscibility of chitin derivatives having monodisperse poly(2-methyl-2-oxazoline) side chains with poly(vinyl chloride) and poly(vinyl alcohol)1," *Macromolecules*, vol. 30, no. 20, pp. 6134–6138, 1997.

[11] T. A. Khan, K. K. Peh, and H. S. Ch'ng, "Mechanical, bioadhesive strength and biological evaluations of chitosan films for wound dressing," *Journal of Pharmacy and Pharmaceutical Sciences*, vol. 3, pp. 303–311, 2000.

[12] V. Singh, D. N. Tripathi, A. Tiwari, and R. Sanghi, "Microwave promoted synthesis of chitosan-graft-poly(acrylonitrile)," *Journal of Applied Polymer Science*, vol. 95, no. 4, pp. 820–825, 2005.

[13] M. Ignatova, N. Manolova, and I. Rashkov, "Novel antibacterial fibers of quaternized chitosan and poly(vinyl pyrrolidone) prepared by electrospinning," *European Polymer Journal*, vol. 43, no. 4, pp. 1112–1122, 2007.

[14] H. Wang, W. Li, Y. Lu, and Z. Wang, "Studies on chitosan and poly(acrylic acid) interpolymer complex. I. Preparation, structure, pH-sensitivity, and salt sensitivity of complex-forming poly(acrylic acid): chitosan semi-interpenetrating polymer network," *Journal of Applied Polymer Science*, vol. 65, no. 8, pp. 1445–1450, 1997.

[15] S.-G. Hu, C.-H. Jou, and M.-C. Yang, "Surface grafting of polyester fiber with chitosan and the antibacterial activity of pathogenic bacteria," *Journal of Applied Polymer Science*, vol. 86, no. 12, pp. 2977–2983, 2002.

[16] D. Mahanta, U. Manna, G. Madras, and S. Patil, "Multilayer self-assembly of TiO_2 nanoparticles and polyaniline-grafted-chitosan copolymer (CPANI) for photocatalysis," *ACS Applied Materials & Interfaces*, vol. 3, no. 1, pp. 84–92, 2010.

[17] M.-Y. Lee, K.-J. Hong, T. Kajiuchi, and J.-W. Yang, "Synthesis of chitosan-based polymeric surfactants and their adsorption properties for heavy metals and fatty acids," *International Journal of Biological Macromolecules*, vol. 36, no. 3, pp. 152–158, 2005.

[18] H. Xia and Q. Wang, "Synthesis and characterization of conductive polyaniline nanoparticles through ultrasonic assisted inverse microemulsion polymerization," *Journal of Nanoparticle Research*, vol. 3, pp. 399–409, 2001.

[19] T. J. Mason and J. P. Lorimer, *Sonochemistry: Theory, Applications and Uses of Ultrasound in Chemistry*, Ellis Horwood, Chichester, UK, 1998.

[20] K. S. Suslick, T. Hyeon, and M. Fang, "Nanostructured materials generated by high-intensity ultrasound: sonochemical synthesis and catalytic studies," *Chemistry of Materials*, vol. 8, no. 8, pp. 2172–2179, 1996.

[21] P. Cintas and J.-L. Luche, "Green chemistry," *Green Chemistry*, vol. 1, no. 3, pp. 115–125, 1999.

[22] M. H. M. Hussein, M. F. El-Hady, W. M. Sayed, and H. Hefni, "Preparation of some chitosan heavy metal complexes and study of its properties," *Polymer Science Series A*, vol. 54, no. 2, pp. 113–124, 2012.

[23] M. H. Hussein, M. F. El-Hady, H. A. H. Shehata, M. A. Hegazy, and H. Hefni, "Preparation of some eco-friendly corrosion inhibitors having antibacterial activity from sea food waste," *Journal of Surfactants and Detergents*, vol. 16, pp. 233–242, 2013.

[24] S. Ramanathan, V. Ponnuswamy, B. Gowtham, K. Premnazeer, and S. C. Murugavel, "Effect of ammonium persulfate (aps) concentration on chitosan grafted polyaniline," *Journal of Optoelectronics and Advanced Materials*, vol. 14, pp. 1011–1015, 2012.

[25] X. H. Xu, G. L. Ren, J. Cheng, Q. Liu, D. G. Li, and Q. Chen, "Self-assembly of polyaniline-grafted chitosan/glucose oxidase nanolayered films for electrochemical biosensor applications," *Journal of Materials Science*, vol. 41, no. 15, pp. 4974–4977, 2006.

[26] R. Karthik and S. Meenakshi, "Removal of Pb(II) and Cd(II) ions from aqueous solution using polyaniline grafted chitosan," *Chemical Engineering Journal*, vol. 263, pp. 168–177, 2015.

[27] A. Yağan, N. Ö. Pekmez, and A. Yildiz, "Electropolymerization of poly (N-methylaniline) on mild steel: synthesis, characterization and corrosion protection," *Journal of Electroanalytical Chemistry*, vol. 578, no. 2, pp. 231–238, 2005.

[28] C.-T. Kuo, S.-Z. Weng, and R.-L. Huang, "Field-effect transistor with polyaniline and poly(2-alkylaniline) thin film as semiconductor," *Synthetic Metals*, vol. 88, no. 2, pp. 101–107, 1997.

[29] B. Narayanasamy and S. Rajendran, "Electropolymerized bilayer coatings of polyaniline and poly(N-methylaniline) on mild steel and their corrosion protection performance," *Progress in Organic Coatings*, vol. 67, no. 3, pp. 246–254, 2010.

[30] A. Tiwari and V. Singh, "Synthesis and characterization of electrical conducting chitosan-graft-polyaniline," *Express Polymer Letters*, vol. 1, no. 5, pp. 308–317, 2007.

[31] J. Wei, Q. Zhang, Y. Liu, R. Xiong, C. Pan, and J. Shi, "Synthesis and photocatalytic activity of polyaniline-TiO_2 composites with bionic nanopapilla structure," *Journal of Nanoparticle Research*, vol. 13, no. 8, pp. 3157–3165, 2011.

[32] S. Sedaghat, "Synthesis and evaluation of chitosan–polyaniline copolymer in presence of ammonium persulfate as initiator," *Journal of Applied Chemical Research*, vol. 8, pp. 47–54, 2014.

[33] A. T. Ramaprasad, V. Rao, G. Sanjeev, S. P. Ramanani, and S. Sabharwal, "Grafting of polyaniline onto the radiation crosslinked chitosan," *Synthetic Metals*, vol. 159, no. 19-20, pp. 1983–1990, 2009.

[34] M. Cabuk, M. Yavuz, and H. I. Unal, "Electrokinetic properties of biodegradable conducting polyaniline-graft-chitosan copolymer in aqueous and non-aqueous media," *Colloids and Surfaces A: Physicochemical and Engineering Aspects*, vol. 460, pp. 494–501, 2014.

[35] W. Zheng, M. Angelopoulos, A. J. Epstein, and A. G. MacDiarmid, "Experimental evidence for hydrogen bonding in polyaniline: mechanism of aggregate formation and dependency on oxidation state," *Macromolecules*, vol. 30, no. 10, pp. 2953–2955, 1997.

[36] Y. Shi, F. Chen, J. Yang, and M. Zhong, "Crystallinity and thermal stability of LDH/polypropylene nanocomposites," *Applied Clay Science*, vol. 50, no. 1, pp. 87–91, 2010.

[37] C.-Y. Hung, C.-C. Wang, and C.-Y. Chen, "Enhanced the thermal stability and crystallinity of polylactic acid (PLA) by incorporated reactive PS-b-PMMA-b-PGMA and PS-b-PGMA block copolymers as chain extenders," *Polymer*, vol. 54, no. 7, pp. 1860–1866, 2013.

[38] J. Joo, Z. Oblakowski, G. Du et al., "Microwave dielectric response of mesoscopic metallic regions and the intrinsic metallic state of polyaniline," *Physical Review B*, vol. 49, no. 4, pp. 2977–2980, 1994.

[39] A. G. MacDiarmid, J. M. Weisinger, and A. J. Epstein, "Advanced research workshop on applications intrinsically conducting polymer," *The Bulletin of the American Physical Society*, vol. 38, p. 311, 1993.

[40] A. G. MacDiarmid and A. J. Epstein, "The concept of secondary doping as applied to polyaniline," *Synthetic Metals*, vol. 65, no. 2-3, pp. 103–116, 1994.

[41] M. Cabuk, Y. Alan, M. Yavuz, and H. I. Unal, "Synthesis, characterization and antimicrobial activity of biodegradable conducting polypyrrole-graft-chitosan copolymer," *Applied Surface Science*, vol. 318, pp. 168–175, 2014.

[42] G. Singh, E. M. Joyce, J. Beddow, and T. J. Mason, "Evaluation of antibacterial activity of ZnO nanoparticles coated sonochemically onto textile fabrics," *Journal of Microbiology, Biotechnology and Food Sciences*, vol. 2, p. 106, 2012.

[43] I. Wiegand, K. Hilpert, and R. E. W. Hancock, "Agar and broth dilution methods to determine the minimal inhibitory concentration (MIC) of antimicrobial substances," *Nature Protocols*, vol. 3, no. 2, pp. 163–175, 2008.